International Journal of Advanced Research in Physical Science (IJARPS)
Volume 3, Issue 7, 2016, PP 34-40
ISSN 2349-7874 (Print) & ISSN 2349-7882 (Online)
www.arcjournals.org

Wavelengths of the 4*d* – 4*p*, 0 – 1 X-ray Laser Transitions in Ni-Like Ions

E. P. Ivanova

Institute of Spectroscopy, Russian Academy of Sciences, Moscow, Troitsk, Russia

Abstract: *The energies of X-ray laser (XRL) transitions in ions of the Ni-like sequence are refined by relativistic perturbation theory with a zero-approximation model potential calculations. The calculated energies of two strongest 4d–4p, J= 0–1 XRL transitions are corrected by extrapolation of the experimental differentials of XRL transition energies $dE_Z^{las} = E_Z^{las} – E_{Z–1}^{las}$; i.e., the differences between transition energies of neighboring ions, which weakly depend on Z (especially, in the region Z ≤ 50). The final results coincide with the known experimental data to within the experimental error. It is shown that the $3d^9_{3/2}4d_{3/2}$ [J = 0]–$3d^9_{3/2}4p_{1/2}$ [J = 1] laser transition with λ = 67.38 nm is possible in Sm^{34+} and the $3d^9_{3/2}4d_{3/2}$ [J = 0]–$3d^9_{5/2}4p_{3/2}$ [J = 1] transition with λ = 67.47 nm is possible in Gd^{36+}. These wavelengths are promising for developing the next generation of photolithography: at present, multilayer mirrors with the reflection coefficient > 60% are designed for this wavelength range.*

1. INTRODUCTION

X-ray laser (XRL) in Ni-like ions was first demonstrated in 1987, where amplification was observed at the wavelengths λ ~ 65.83 and ~71 Å on J = 0-1, *4d - 4p* transitions [1] in europium laser plasma (Eu^{35+}). Later a series of results demonstrating amplification at the wavelengths of these transitions in Yb^{42+} were obtained [2]. Amplification in laser plasma of tantalum (Ta^{45+}) and tungsten (W^{45+}) in the "water window" boundary region with λ~ 44.8 Å and λ ~ 43.2 Å, respectively, was detected in 1990 in [3]. The shortest wavelength of ~35.6 Å of the Ni-like XRL series was recorded in Au^{51+} [4]. In the theoretical study [5], the energies of *4d –4p* transitions in the Ni-like XRL series were calculated using the relativistic multiconfigurational Hartree-Fock method. Some possible laser lines were predicted in [5] for ions with Z = 46 – 92. The wavelengths were determined by fitting *ab initio* calculations to the known experimental wavelengths followed by interpolation and extrapolation to the region of small nucleus charges to Z = 46. In [6], the wavelengths of Ni-like XRLs with low Z were measured in the range *39< Z < 49*. Later in [7], Ni-like ion spectra were theoretically and experimentally analyzed, the wavelengths of the $3d^94d\ ^1S_0 – 3d^94p\ ^1P_1$ laser transitions in ions Y^{11+} – Mo^{14+} were refined, and these transitions in As^{5+}, Br^{6+}, and Rb^{9+} ions were identified for the first time. The review of the sequential development of the XRL engineering since the very first experiments, their development motivation in view of possible applications was published in [8], where all experimental XRL wavelengths determined by that time for Ne- and Ni-like ions were presented.

In this paper we refine the theoretical data [5] for two $3d^94d$ [J = 0]–$3d^94p$ [J = 1] laser transitions in Ni-like ions with $Z \le 79$; the refinement is possible because of the use of high-precision energies of XRL transitions at initial points of the sequence for Z = 36–48 [6,7]. We extrapolate the differentials of transition energies $E_Z^{las} – E_{Z–1}^{las}$, i.e., the differences between transition energies of neighboring ions, which weakly depend on Z (especially, in the region $Z \le 50$). The calculation will allow us to determine the ions for which the XRL wavelengths lie in the range of 67.0–67.5 Å. These wavelengths are promising for developing the next generation of photolithography: at present, multilayer mirrors with the reflection coefficient > 60% are designed for this wavelength range [9].

2. ENERGY OF THE UPPER ACTIVE LEVEL E2 ALONG THE ISOELECTRONIC SEQUENCE

The Ni-like scheme of an XRL is shown in Fig. 1, there are other XRL transitions in heavy ions which are not considered here. The inversion is due to strong collisional excitation of the $3d^94d$ [J = 0] upper working level by electron impact and rapid radiative depletion of the $3d^94p$ [J = 1] lower working level. Two $3d^94d$ [J = 0] levels denoted by $E1$ and $E2$ are shown in Fig. 1.

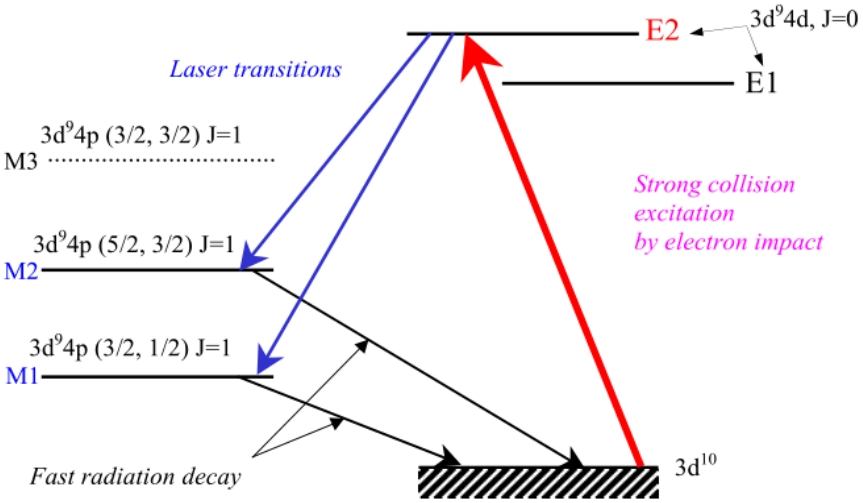

Figure1. *Two principal XRL transition in Ni-like ions*

The working XRL level is denoted by $E2$, it lies above the $E1$ level along the isoelectronic sequence. In Ni-like ions there are three rapidly decaying (resonant) levels of the $3d^9 4p$ configuration denoted as $M1$, $M2$, and $M3$. The $M2$ level is the lower working level of an XRL for the entire nickel isoelectronic sequence, the $M1$ level is the lower working level for heavy ions starting with $Z = 62$. The $M3$ level decays to the ground state significantly weaker than $M1$ and $M2$; therefore, the gain on the $E2$–$M3$ transition is weak and is not considered here.

Table. *The wavelengths of two laser transitions E2 – M2 and E2 – M1 (Å) in Ni- like ions, calculated in the present work for comparison with data of [5,6], the experimental wavelengths [6,8] are also given.*

	E2 – M2				*E2 – M1*		
Z	Present Work	Theory [6]	Theory [5]	Exp. [6,8]	Present work	Theory [5]	Exp. [8]
46 Pd	146.77	146.5	148.10	146.8	142.24	142.93	
47 Ag	138.92	138.6	139.92	138.9	134.42	135.07	
48 Cd	131.65	131.4	132.56	131.7	127.27	127.93	
49 In	125.34	124.9	125.89	125.8	120.88	121.42	
50 Sn	119.00	119.0	119.82	119.7	114.80	115.44	
51 Sb	113.70	113.6	114.25		109.27	109.93	
52 Te	108.52	108.7	109.14	111.0	104.13	104.83	
53 I	103.71	103.9	104.40		99.32	100.09	
54 Xe	99.10	99.65	100.2	99.8	94.71	95.66	96.4
55 Cs	94.92	95.64	95.93		90.50	91.53	
56 Ba	91.03	91.90	92.12		85.56	87.65	
57 La	87.43	88.40	88.55	89.0	82.88	83.99	
58 Ce	84.04	85.10	85.19	86.0	79.42	80.55	
59 Pr	80.85	82.00	82.03	82.0	76.15	77.29	
60 Nd	77.84	79.06	79.05	79.2	73.06	74.20	
61 Pm	75.03		76.23		70.22	71.27	
62 Sm	72.37		73.55	73.60	67.38	68.49	68.50
63 Eu	69.82		71.00	71.00	64.90	65.83	65.83
64 Gd	67.47		68.58	68.60	62.47	63.30	63.33
65 Tb	65.36		66.26	67.00	60.22	60.88	59.00
66 Dy	63.34		64.06	64.10	58.07	58.57	58.5
67 Ho	61.35		61.94	62.00	55.91	56.36	56.3
68 Er	59.38		59.92		53.79	54.23	
69 Tm	57.45		57.98		51.77	52.20	
70 Yb	55.57		56.11	56.09	49.80	50.24	50.26
71 Lu	53.78		54.32		47.94	48.36	
72 Hf	52.06		52.60		46.11	46.55	46.50

73 Ta	50.39		50.94		44.38	44.82	44.80
74 W	48.80		49.35		42.71	43.14	43.20
75 Re	47.29		47.81		41.10	41.53	
76 Os	45.82		46.32		39.59	39.98	
77 Ir	44.40		44.88		38.12	38.48	
78 Pt	43.10		43.50		36.72	37.04	
79	41.77		42.16		35.30	35.65	35.6

Comparison of the theoretical [5] and experimental [6, 8] results presented in the table shows significant discrepancies between these results in the region Z = 46–49. This is explained by the fact that the wavelengths and gains in the light Ni-like ions were measured after the extrapolation to the region of small Z was performed in [5].

These notations of working levels were introduced in one of the first calculations of atomic characteristics of Ni-like ions [10]. The reason is that, in the *jj*-coupling scheme for angular momenta used here, the classification of levels $E2$ and $E1$, changes along the sequence.

Figure 2a shows the experimental XRL wavelengths of a Ni-like sequence for transitions $E2$–$M2$ and $E2$–$M1$, which can be represented by smooth curves. Figure 2b shows the differentials of transition energies for neighboring Z-points $dE_Z^{las} = E_Z^{las} - E_{Z-1}^{las}$ (the value of differential is shown at the middle

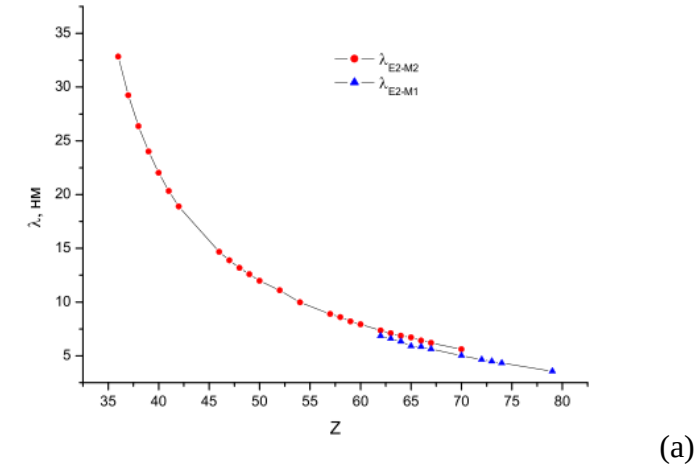

(a)

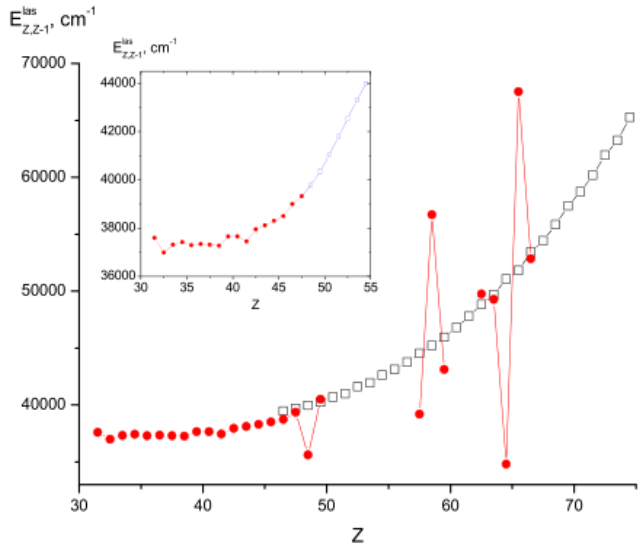

(b)

Fig.2. ***(a)*** *Experimental XRL wavelengths in the Ni-like ions: E2–M2 (circles), E2–M1 (triangles).*
(b) *Z-dependence of differentials of the E2–M2 transition energy: $E^{las}_{Z,,Z-1} = E^{las}_{Z} - E^{las}_{Z-1}$ (solid circles show the data from review [8], squares are the calculated results [5]). The inset shows the extrapolation of differentials from the plot for $Z < 49$ to the region of $Z = 55$. Solid circles are the differentials derived from experiments, empty circles are extrapolated results.*

Point between Z and $Z - 1$). The squares show the values of $dE^{las}_{Z,Z-1}$ obtained from the data calculated in [5]. There are three intervals of Z where the $E2$–$M2$ transition energies were measured for each following value of Z: $31 \le Z \le 50$ [6, 8], $57 \le Z \le 60$ and $62 \le Z \le 67$ [8].

The values of dE_Z^{las} for the transition energies in the region $36 \le Z \le 48$ measured in [6,7] are represented by a smooth function (see Fig. 2b), which is indicative of a high accuracy of measurements for low values of Z with the transition energies inaccurate in the fourth significant figure. The values of differentials in the two other intervals demonstrate strong spikes. This suggests that the measurements of the corresponding XRL wavelengths for ions with large nuclear charges may be inaccurate and an additional consideration (improvement) is necessary.

The problem of extrapolation of the $E2$–$M2$ and $E2$–$M1$ transition energies lies in the difficulty of calculating the upper $E2$ level—the $^1S_0$ state in the LS-coupling scheme for the angular momenta. For this reason, the data for the $J = 0$ energy levels are absent in some detailed calculations of atomic constants of Ni-like ions [11]. The problem of an anomalously large error of the calculation of the $3d4d$ [$J = 0$] level in Ni-like ions was discussed in our previous paper [12]. In our approach it is connected with an insufficient accounting for the second-order correlation corrections of a perturbation theory in the interelectronic interaction, which insignificantly vary along the sequence. In addition, the insufficient consideration of relativistic interaction corrections can lead to a more complicated Z dependence of corrections not taken into account. The energies of lower working levels $3d^9 4p$ [$J = 1$] $M1$, $M2$, $M3$ and the rates of their depletion are calculated with a good accuracy in different theoretical approaches [10–14], and their experimental high Z energies (69-83) are collected in [14] for comparison with our calculations [14].

The general principles of the method of the relativistic perturbation theory with a zero-approximation model potential (RPTMP) for calculations of energy levels and probabilities of transitions to the ground state of atomic systems with a filled ground state shell are presented in [12]. Here we use this method to calculate the energy levels $E1$, $E2$, $M1$, $M2$, and $M3$ for the ions of a Ni-like sequence with $Z = 36$–79. The main purpose is to determine the correction $\Delta E_{corr}(Z)$ to a value $E2_{\text{in}}$ calculated by the RPTMP method for each Z: $E2 = E2_{\text{in}} + \Delta E_{corr}$. To do this, we use the high-precision experimental values of transition energies $E2 - M2 = E^{\text{las}}$ for $Z = 36$–48 from [6] and the well-known $M2$ energy values [15]. To determine ΔE_{corr}, we extrapolate the differential $dE_Z^{las} = E_Z^{\text{las}} - E_{Z-1}^{\text{las}}$, shown in the inset in Fig. 2b, to a value of $Z = 55$. Starting with $Z = 49$, we determine E_Z^{las}, ΔE_{corr}, and $E2$ from the values of differentials. $\Delta E_{corr}(Z)$ is shown in Fig. 3 as a function of Z. Note that with the $E2$ values thus determined the values of E^{las} and λ^{las} for Z up to 55 coincide with a good accuracy with the theoretical extrapolation of XRL wavelengths performed in [6]. One can see in Fig. 3 that extrapolation from $Z = 55$ to the region of $Z \sim 65$ is evident. Extrapolation to the region of $Z = 79$ is performed using the experimental measurements of the $E2$–$M1$ transition for $Z > 72$.

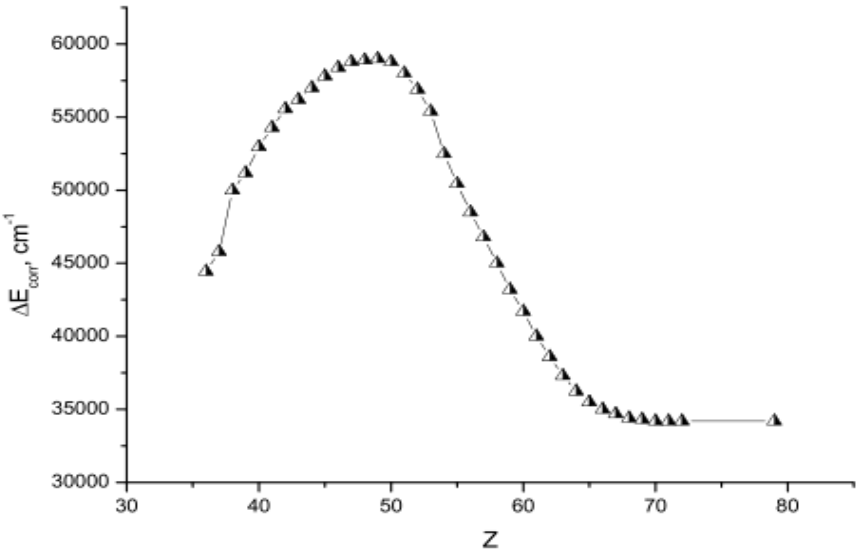

Fig3. *Z-dependence of the correction ΔE_{corr} to the calculated $E2_{in}$ energy*

The *E*1 energy values for the sequence are calculated with a good accuracy. This was demonstrated in [12] and also follows from comparison with the available experimental measurements [15].

The correction function ΔE_{corr} to the calculated $E2_{in}$ level has a maximum at $Z \sim 51$ (Fig. 3). Practical calculations of energy levels of ions along isoelectronic sequences show that the neglected correlation corrections of the second and higher orders weakly change along the sequence. This allows semiempirical extrapolation methods to be developed [16]. The difficulty encountered in calculating the *E*2 energy along the Ni-like sequence is the presence of a significant extremum in the function ΔE_{corr} (Fig. 3). The nature of this extremum is connected with a strong coupling between the *E*1 and *E*2 states. In the zero order approximation, these states are quasi-degenerated, with the *E*2 state lying below the *E*1 state. The first-order and (partially) higher-order corrections remove the degeneracy and change the positions of levels so that the *E*2 level becomes the upper level. The correction to the calculated $E2_{in}$ level is ~ 52 000 cm^{-1} for $Z = 36$ and increases with *Z*, which suggests that the role of second-order correlation corrections ignored in the calculation becomes more important. The correction reaches its maximum value of ~ 58 000 cm^{-1} at $Z = 51$. It follows from Fig. 3 that the coupling energy of levels *E*1 and *E*2 increases with *Z*. This is seen in Fig. 4a which presents the contributions of levels *E*1 and *E*2 (the squares of elements of the corresponding eigenvector) to the upper working *E*2 level along the isoelectronic sequence of Ni-like ions. For $Z \leq 51$, the $3d_{5/2}4d_{5/2}$ [$J = 0$] state is dominant in the

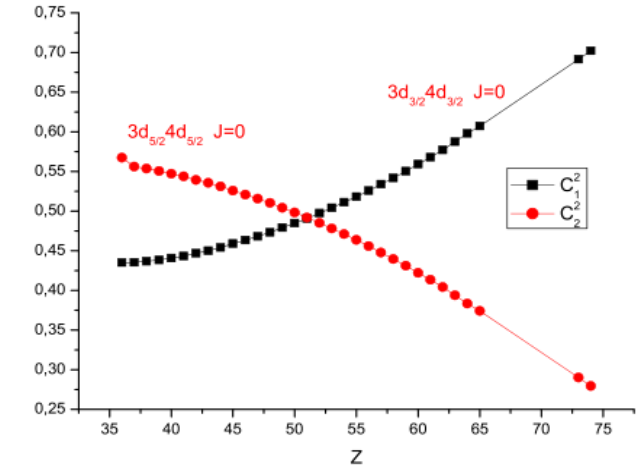

(a)

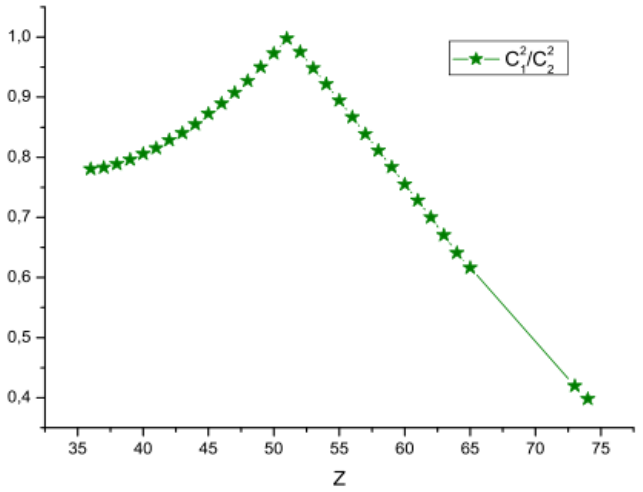

(b)

Fig4. ***(a)*** *Contributions of levels (1) E1 and (2) E2 (the squares of elements of the corresponding eigenvector C^2) to the upper working level E2 along the isoelectronic sequence of Ni-like ions. For $Z \leq 51$, the $3d_{5/2}4d_{5/2}$ [$J = 0$] state is dominant in the classification of the E2 level, and the $3d_{3/2}4d_{3/2}$ [$J = 0$] state is dominant for $Z > 51$.* ***(b)*** *Ratio of contributions of the lower and upper 3d4d [J = 0] levels to the active upper E2 level as a function of Z.*

Classification of the $E2$ level, while the $3d_{3/2}4d_{3/2}$ [$J = 0$] state is dominant for $Z > 51$. At $Z = 51$ (at the point of a maximum) the quantum numbers in the classification of levels $E2$ and $E1$ are interchanged. As Z increases further, the coupling of levels decreases; Fig. 4b shows the ratio of contributions (the squares of eigenvectors) of lower and upper levels $E1$ and $E2$ to the active upper $E2$ level. At $Z = 67$ the function ΔE_{corr} (Fig. 3) bends and tends to an asymptotic constant value. This part of the curve of ΔE_{corr} is in agreement with the experimental data [2, 3] and the calculation [5].

Such strong interaction of levels is the characteristic of calculations within the *jj*-coupling scheme for the angular momenta; in another basis set, for example, in the *LS*-scheme, the $E1$ and $E2$ states have practically no admixtures. However, the problem of anomalously low accuracy of the $E2$ energy level is also present in *LS*-scheme and is also explained by the weak convergence of a perturbation theory series.

The wavelengths λ_{las} of laser transitions $E2$–$M2$ and $E2$–$M1$ obtained in our calculation are summarized in the table. They are compared to the calculated/extrapolated values of [5, 6] and the experimental results of [6, 8]. The first XRLs in the Ni-like sequence were observed in heavy ions with $Z = 63, 73, 74, 79, \ldots$, where the error of measurement of λ_{las} was estimated to be ±0.03 nm. On this basis a correct extrapolation to the region of smaller Z was carried out. Subsequently, after special studies of XRLs in the ions of Ag, In, Sn, and Sm [17] the error of measurement became 0.1 nm ~ 1 Å. As a result, as one can see from the first rows of the table, the discrepancy between the wavelengths calculated in [5] and obtained in the precision experiment [6] exceeds 1 Å. It is possible that the accuracy of measurement of λ_{las} in the first experiments was overestimated. It seems likely that significant errors in measuring λ_{las} were also observed in other experiments [18], the wavelengths of which are interpreted in Fig. 2b. Note that the values of λ_{las} obtained by extrapolation in [6] are in good agreement with the experimental data in the region of $Z < 55$, and they are close to the calculated results [5] for $Z > 55$.

3. CONCLUSION

It was possible to construct the curve of corrections $\Delta E_{\text{corк}}$ (Fig. 3) to the calculated $E2_{in}$ level values due to the presence of the precision values of λ_{las} in the region of $36 \le Z \le 48$ [6], which allowed us to perform extrapolation with a good accuracy to the region $Z \sim 60$–65. Further the curve ΔE_{corr} tends to an asymptotic value in conformity with the experiments [2, 3].

Determination of the Ni-like ions with λ_{las} lying within the range of 6.7–6.75 nm is the important result of this calculation. It is exactly this range for which normal-incidence multilayer mirrors are being developed at present on the basis of pairs B/La and B4C/La, which are promising for lithography of the next generation [9]. The reflection curves were calculated in [9] for different types of multilayer pairs, some of which exhibit the reflection coefficient exceeding 65%. One can see in the table that $\lambda_{\text{las}} = 6.738$ nm in Sm^{34+} on the *E2 – M1* transition and $\lambda_{\text{las}} = 6.747$ nm in Gd^{36+} on the *E2 – M2* transition. These values coincide with the experimental results to within the experimental error.

REFERENCES

[1] MacGovan B J *et al* 1987 *Phys. Rev. Lett.* **59** 2157-60.

[2] MacGovan B J, Maxon S, Kean C J, London R A, Matthews D L and Whelan D A 1988 *J. Opt. Soc. Am.* B **5** 1858-1863

[3] MacGovan B J *et al* 1990 *Phys. Rev. Lett*. **65** 420-423.

[4] MacGovan B J *et al* 1992 *Phys. Fluids* B **4**.2326-37

[5] Scofield J H and MacGovan B J 1992 *Physica Scripta* **46** 361-364

[6] Li Yu, Nilsen J, Dunn J, Osterheld A L, Ryabtsev A and Churilov S S 1998 *Physical Review* A **58** R2668-71

[7] Ryabtsev A N, Churilov S S, Nilsen J, Li Yu, Dunn J, Osterheld A L 1999 *Optics and Spectroscopy* **87** 197-202 (Russian)

[8] Daido H 2002 *Pep. Prog. Phys.* **65** 1513-76

[9] Makhotkin I.A, Zoethout E., Van de Cruijs R., Yakunin S.N., Louis E., Yakunin A.M., Banine V., Müllender S., and Bijkerk F. 2013 *OPTICS EXPRESS* **21** 29894

[10] Zhang H L, Sampson DH 1989 *At. Data Nucl. Data Tables* **43** 1-

[11] Safronova U I, Safronova A S, Hamasha S M, Beiersdorfer P 2006 *At. Data and Nucl. Data Tables* **92** 47-104

[12] Ivanova E P 2014 *Optics and Spectroscopy* **117** 167-175

[13] Aggarwal K M, Norrington P H, Bell K L, Keenan F P, Pert G J, Rose S J 2000 *At. Data Nucl. Data Tables* **74** 157-255

[14] Gogava A.L., Ivanova E.P. 1985 *Optics and Spectroscopy* **59** 1310-1315

[15] Ryabtsev A.N., Churilov S.S. in *Spectroscopy of Multiple Charged Ions in Plasmas* (Nauka, Moscow, 1991) p. 76-114 [in Russian]

[16] Ramonas A. *Semiempirical Atomic Spectroscopy* (Technika, Vilnus 2000)

[17] Lin J.Y. *et al* 1998 *Opt. Commun.* **158** (1-6) 55-60

[18] Daido et al 1999 *J. Opt. Soc. Am.* B **16** 296-300